Süleyman Demirel Üniversitesi
Fen Bilimleri Enstitüsü Dergisi
Cilt 29, Sayı 2, 407-414, 2025

Süleyman Demirel University
Journal of Natural and Applied Sciences
Volume 29, Issue 2, 407-414, 2025

DOI: 10.19113/sdufenbed.1667586

Synthesis, Structural Analysis and Comparison with Theoretical Calculations of Heterocyclic Disperse Diazo Dyes

Aykut DEMİRÇALI*

Pamukkale Universty, Faculty of Science, Department of Chemistry, 20160, Denizli, Türkiye

(Alınış / Received: 28.03.2025, Kabul / Accepted: 21.07.2025, Online Yayınlanma / Published Online: 25.08.2025)

Keywords
Azo dye,
Spektral analysis,
Density Functional Theory

Abstract: The interest in azo dyes is increasing in the textile and dye industry. Along with this interest, in addition to experimental studies, quantum mechanical calculations have recently been frequently encountered in the literature. In the content of the study, first of all, three azo dyes are synthesized. Then, the characteristic properties of the compounds are determined experimentally using FT-IR, ^{1}H-NMR and ^{13}C-NMR spectroscopies. Then, the compounds are optimized in the B3LYP/6-311+(d,p) basis set using density functional theory with the Gaussian16 program. Theoretically, FT-IR and ^{1}H-NMR values are calculated. It is observed that the experimental and theoretical results are compatible. In addition, the electronic properties of the azo dyes are investigated.

Heterosiklik Dispers Diazo Boyalarının Sentezi, Yapısal Analizi ve Teorik Hesaplamalarla Karşılaştırılması

Anahtar Kelimeler
Azo boyarmadde,
Yapı analizi,
Yoğunluk Fonksiyonel Teorisi

Öz: Azo boyar maddelere olan ilgi tekstil ve boya endüstrisinde giderek artmaktadır. Bu ilgiyle beraber, deneysel çalışmalara ek olarak kuantum mekaniksel hesaplamalara da son zamanlarda literatürde sıklıkla rastlanmaktadır. Çalışmanın içeriğinde öncelikle üç adet azo boyar madde sentezlenmiştir. Devamında bileşiklerin karakteristik özellikleri önce FT-IR, ^{1}H-NMR ve ^{13}C-NMR spektroskopileri kullanılarak deneysel olarak belirlenmiştir. Sonra Gaussian16 programıyla yoğunluk fonksiyonel teorisi kullanılarak bileşikler B3LYP/6-311G(d,p) baz setinde optimize edilmiştir. Teorik olarak, FT-IR ve ^{1}H-NMR değerleri hesaplanmıştır. Deneysel ve teorik sonuçların uyumlu olduğu gözlenmiştir. Bunlara ilave olarak, azo boyar maddelerin elektronik özellikleri incelenmiştir.

1. Introduction

Azo dyes are synthetic compounds that have revolutionized industrial dyeing processes and offer a wide range of colors. The main feature of azo dyes is the presence of an azo group (-N=N-) in their molecules. This group acts as a chromophore group that determines the color properties of the dye.

They are produced by chemical processes called diazotization and coupling reactions. These processes involve the reaction of aromatic amines with nitrous acid to form diazonium salts, which are then reacted with other aromatic compounds to form azo dyes [1-3].

Azo dyes are widely used in many sectors such as biochemistry, medicine, food and beverage, pharmaceutical, printing inks, plastics, leather and textile and paint industries due to their high color intensity, vivid and bright colors, wide color range, economical production and suitability for various application methods [4].

Some azo dyes are used in biochemical tests to detect and measure biomolecules such as proteins, enzymes and DNA [5-7] and due to their structure, they can form complexes with metal ions. Thus, they have the ability to change the color properties of the dye and increase the performance of dyes in textile, paint and other industrial applications [8,9].

* Corresponding author: ademircali@pau.edu.tr

These compounds are widely preferred in the textile industry due to their high affinity and good fastness properties in the dyeing of synthetic fabrics such as nylon, polyester and polyamide [10,11]. They are also used in the leather industry in the coloring of leather products. Because they provide deep and permanent colors to leather products and maintain the flexibility and durability of the leather [12,13].

In addition, since they provide vivid and bright colors in printing inks, they are used in printing on various surfaces such as paper, plastic and metal with techniques such as offset printing and digital printing [14,15].

In recent years, theoretical investigations of chemical compounds have considerable attention due to their intriguing electronic and geometric properties, particularly their potential applications [16]. The present study analyzed the molecular structures, vibrational modes, and NMR spectra of disazo dyes 3a–c using quantum chemical methods at the DFT level with the 6-311G(d,p) basis set. The comparison between experimental data and theoretical results plays a crucial role in the accurate assignment and deeper understanding of vibrational and NMR spectra, as well as the molecular structures of these compounds.

In this study, three disperse disazo dyes containing pyrazole and coumarin are synthesized based on aniline, p-chlorine aniline and p-methyl aniline compounds. Then, the structures of the synthesized compounds are elucidated using various spectroscopic methods and compared with theoretical calculations.

2. Material and Method

All consumables used throughout the study are pure and imported products.

The following devices are used in the structural analysis of the obtained dyes and in the necessary spectroscopic analyses, respectively. It is measured melting points in Electrothermal 9100 melting point determination device and elemental analysis in Costech ECS 4010 device. Structure analysis of compounds is analyzed spectrometric methods such as FT-IR analyses in Perkin Elmer Spectrum Two spectrophotometer, ^{13}C and proton NMR spectra in a 400 MHz Varian NMR device.

2.1. Synthesis of (4'-phenylazo-3'-amino-1'H-pyrazol-5'-ylazo)-4-hydroxy coumarin (aa3a)

0.01 mol aniline is dissolved in sufficient amount of HCl. $NaNO_2$ aqueous solution is added very slowly on this solution and is stirred in an ice bath for 4 hours. Formed the diazonium salt is added to 0.01 mol malononitrile solution prepared in another beaker and is stirred in an ice bath for another 4 hours. 3,5-diamino-4-phenylazo-1H-pyrazole (aa2a) compound is synthesized [3]. aa2a compound is filtered, is dried and is crystallized in DMSO solvent. Afterwards, aa2a dye is dissolved in 20 ml acetic acid and 20 ml HCl mixture and 0.015 mol $NaNO_2$ aqueous solution is added and is stirred for 4 hours. At the end of the period, formed the diazonium salt is added to the solution of 0.01 mol 4-hydroxy coumarin formed in NaOH and water mixture and left to stir for another 4 hours. The final product (4'-phenylazo-3'-amino-1'H-pyrazol-5'-ylazo)-4-hydroxy coumarin (aa3a) is filtered, air is dried and is purified in DMSO solvent. Mol. formula: $C_{18}H_{13}N_7O_3$; Mol. weight: 375 g/mol; Color: orange crystal; Yield: 75 %; mp 333–334 ^oC. Elemental analysis, Found, %: C: 60.41, H: 3.58, N: 27.39; Calculated, % C: 60.17, H: 3.62, N: 27.30.

2.2. Synthesis of [4'-(4''-chlorophenyl)azo-3'-amino-1'H-pyrazol-5'-ylazo]-4-hydroxy coumarin (aa3b)

0.01 mol 4-chloro aniline is dissolved in sufficient amount of HCl. $NaNO_2$ aqueous solution is added very slowly on this solution and is stirred in an ice bath for 4 hours. Formed the diazonium salt is added to 0.01 mol malononitrile solution prepared in another beaker and is stirred in an ice bath for another 4 hours. 3,5-diamino-4-(4'-chlorophenyl)azo-1H-pyrazole (aa2b) compound is synthesized [3]. aa2b compound is filtered, is dried and is crystallized in DMSO solvent. Afterwards, aa2b dye is dissolved in 20 ml acetic acid and 20 ml HCl mixture and 0.015 mol $NaNO_2$ aqueous solution is added and is stirred for 4 hours. At the end of the period, formed the diazonium salt is added to the solution of 0.01 mol 4-hydroxy coumarin formed in NaOH and water mixture and left to stir for another 4 hours. The final product 4'-(4''-chlorophenyl)azo-3'-amino-1'H-pyrazol-5'-ylazo]-4-hydroxy coumarin (aa3b) is filtered, air is dried and is purified in DMSO solvent. Mol. formula: $C_{18}H_{12}N_7ClO_3$; Mol. weight: 409.5 g/mol; Color: brown crystal; Yield: 82 %; mp 341–342 ^oC. Elemental analysis, Found, % C: 54.86, H: 3.11, N: 24.76; Calculated, %: C: 54.89, H: 3.05, N: 24.90.

2.3. Synthesis of [4'-(4''-methylphenyl)azo-3'-amino-1'H-pyrazol-5'-ylazo]-4-hydroxy coumarin (aa3c)

0.01 mol 4-methyl aniline is dissolved in sufficient amount of HCl. $NaNO_2$ aqueous solution is added very slowly on this solution and is stirred in an ice bath for 4 hours. Formed the diazonium salt is added to 0.01 mol malononitrile solution prepared in another beaker and is stirred in an ice bath for another 4 hours. 3,5-diamino-4-(4'-methylphenyl)azo-1H-pyrazole (aa2c) compound is synthesized [3]. aa2c compound is filtered, is dried and is crystallized in DMSO solvent. Afterwards, aa2c dye is dissolved in 20 ml acetic acid and 20 ml HCl mixture and 0.015 mol $NaNO_2$ aqueous

solution is added and is stirred for 4 hours. At the end of the period, formed the diazonium salt is added to the solution of 0.01 mol 4-hydroxy coumarin formed in NaOH and water mixture and left to stir for another 4 hours. The final product 4'-(4''-methylphenyl)azo-3'-amino-1'H-pyrazol-5'-ylazo]-4-hydroxy coumarin (aa3c) is filtered, air is dried and is purified in DMSO solvent. Mol. formula: $C_{19}H_{15}N_7O_3$; Mol. weight: 388 g/mol; Color: light yellow crystal; Yield: 71 %; mp 322–323 °C. Elemental analysis, Found, % C: 61.22, H: 4.09, N: 26.18; Calculated, %: C: 61.13, H: 4.02, N: 26.27.

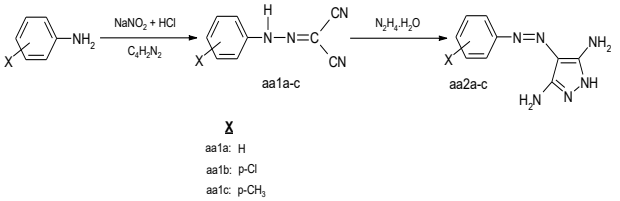

Scheme 1. Synthesis of aa2a-c dyes

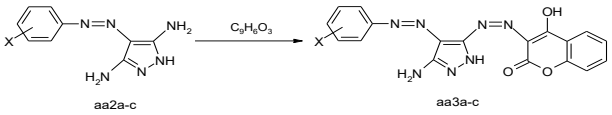

Scheme 2. Synthesis of aa3a-c dyes

2.4. Theoretical calculations

One of the most successful quantum chemistry tools for describing the ground state properties of chemical compounds is hybrid density functional theory (DFT). Here, the most stable states of the synthesized azo dyes are calculated using DFT and the obtained results are in convincing agreement with the experimental data [17–19]. The molecular structure of the compound are optimized to obtain global minima using the B3LYP/6-311G(d,p) level [20–22]. After that, the same basis set and computational method are used for FT-IR and ^{1}H-NMR spectra of the compound using the optimized structure. All calculations are performed in the gas phase using the Gaussian 16. Rev. B1 program [23]. GaussView 6.0 is also used for visualization of the structure [24].

3. Results

3.1. Basic properties

The aim of our study is to introduce disperse disazo dyes that can dye nylon and polyester fabrics to the literature for the dye and textile industry. The basic properties of the three synthesized disazo dyes are given in sections 2.1, 2.2 and 2.3. When the results are examined, it is seen that bright colors such as orange, brown and light yellow are obtained. The highest yield is obtained in compound aa3b, while the lowest yield is obtained in compound aa3c. It can be thought that this situation is due to the fact that the chlorine group attached to the phenyl ring facilitates the formation of the diazo compound by withdrawing electrons from the ring. Similarly, it can be said that the reason for the low yield of compound aa3c is that the methyl group attached to the phenyl ring provides electrons to the ring and makes the formation of the diazo compound difficult.

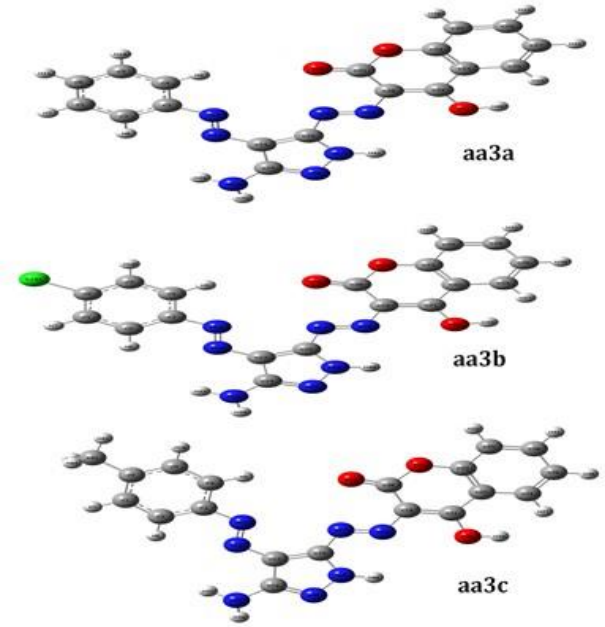

Figure 1. Optimized geometry for aa3a-c compounds calculated at DFT/B3LYP/6-311G(d,p) level.

3.2. Tautomerism

When the structures of aa3a, aa3b and aa3c compounds are examined, it is determined that the dyes could be in 3 different tautomeric forms. These are disazo-keto (T1), disazo-enol (T2) and azo-hydrazo keto (T3) forms. According to FT-IR data, all synthesized dyes are in disazo-keto form, while according to ^{1}H-NMR data, they are converted to disazo-enol form in DMSO-d_6.

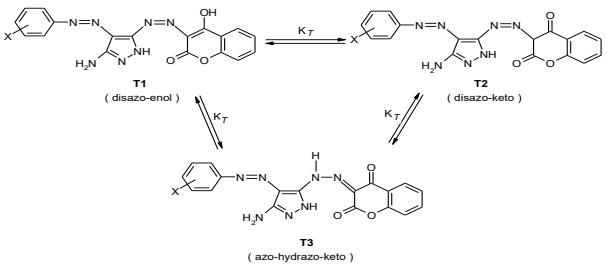

Scheme 3. Tautomeric structures of aa3a-c dyes

3.3. Structure analysis

FT-IR, ^{1}H-NMR and ^{13}C-NMR analyses are performed to elucidate the structures of the synthesized compounds. The obtained data are summarized in Table 1, Table 2 and Table 3. In addition, sample spectra of these analyses are shown in Figure 2, Figure 3, Figure 5, Figure 6, Figure 8 and Figure 9. Also, the spectrum showing the correlation calculation of theoretical and experimental data of FT-IR spectroscopy is given in Figure 4.

Table 1. FT-IR data for azo dyes aa3a-c

Dye No	aa3a		aa3b		aa3c	
	Cal.	Exp.	Cal.	Exp.	Cal.	Exp.
ν_{NH2}	3423	3357	3423	3361	3424	3358
ν_{NH}	3272	3224	3271	3283	3274	3241
ν_{Aro-H}	3159 3112 3059	3166 3109 3071	3157 3084	3141 3073	3165 3094	3184 3075
ν_{Alip-H}	-	-	-	-	2957	2838
$\nu_{C=O}$	1721 1640	1729 1647	1715 1668	1730 1650	1711 1673	1728 1650
$\nu_{N=N}$	1464 1455	1479 1460	1512 1484	1520 1462	1518 1467	1520 1457
ν_{C-O-C}	1237	1203	1238	1204	1233	1204

When Table 1 is examined, two separate -N=N- (azo) peaks were observed in the range of 1457-1520 cm^{-1} for each dye. Two -C=O (carbonyl) peaks are determined in the range of 1647-1730 cm^{-1}. In addition, $-NH_2$ peaks are determined in the range of 3357-3361 cm^{-1} and -NH peaks are determined in the range of 3224-3283 cm^{-1}. The presence of two separate azo and carbonyl peaks in the structural analysis indicates that the synthesized dyes are in the disazo keto (T2) tautomeric form in the solid state.
When the theoretical calculation data are examined, the -N=N- (azo) peaks in the range of 1455-1518 cm^{-1} and two C=O peaks in the range of 1640-1721 cm^{-1} show that the compounds are in the disazo keto (T2) form in the theoretical calculations as well as in the experimental results.
Both the experimental results and the theoretical calculations confirm each other.

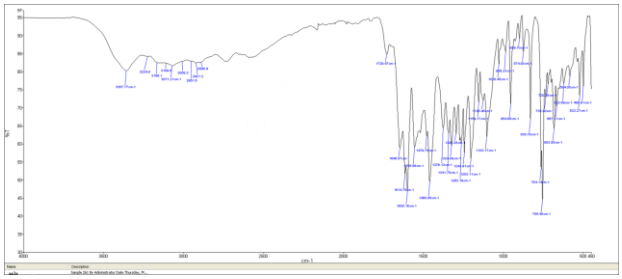

Figure 2. FT-IR spectra of aa3a dye.

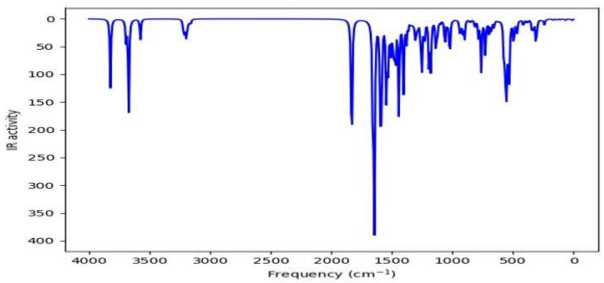

Figure 3. The calculated spectra FT-IR of aa3a.

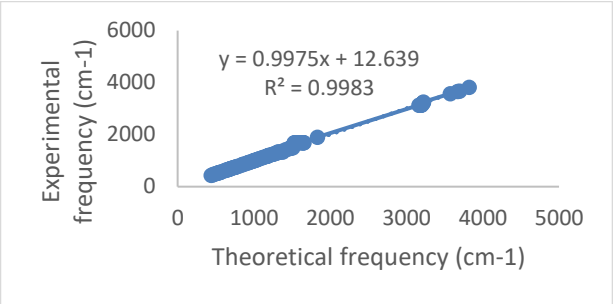

Figure 4. The correlation graphs between the experimental and calculated frequencies for the dye aa3a.

When ^{1}H-NMR data of all synthesized compounds are examined, aromatic hydrogen peaks are observed in the range of 7.11-8.11 ppm. Peaks are observed in the range of 12.95-13.42 ppm belonging to the OH group attached to the coumarin compound, in the range of 13.53-14.49 ppm belonging to the NH group attached to the pyrazole ring, and in the range of 5.39-5.48 ppm belonging to the NH_2 group attached to the pyrazole ring. In addition, the aliphatic hydrogen peak belonging to the CH_3 group attached to the phenyl ring in the aa3c compound is observed at the level of 1.17 ppm. Similarly, as a result of theoretical calculations, aromatic hydrogen peaks are observed in the range of 7.88-8.70 ppm, OH peaks in the range of 6.75-6.88 ppm, NH peaks in the range of 9.70-9.82 ppm and NH_2 peaks in the range of 4.91-4.98 ppm.

Both experimental and theoretical results are consistent with each other and show that the synthesized dyes are in disazo enol (T1) tautomeric form in DMSO-d6 solvent.

Table 2. ^{1}H-NMR data for dyes aa3a-c

Dye No	aa3a		aa3b		aa3c	
	Cal.	Exp.	Cal.	Exp.	Cal.	Exp.
Ar-H	7.89-8.70	7.13-7.94	7.88-8.64	7.33-7.84	7.94-8.52	7.11-8.11
Al-H	-	-	-	-	1.93	1.17
O-H	6.88	13.42	6.75	12.95	6.83	13.22
NH	9.70	14.49	9.82	13.53	9.78	13.54
NH_2	4.91	5.39	4.98	5.48	4.94	5.47

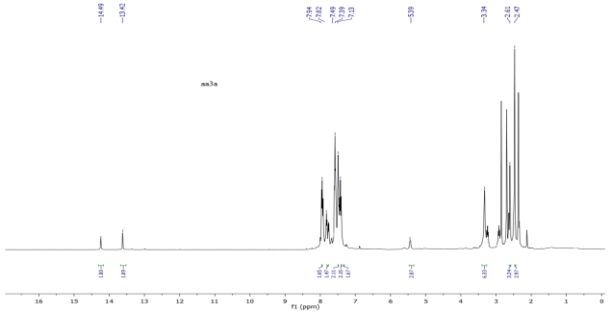

Figure 5. ^{1}H-NMR spectra of aa3a dye.

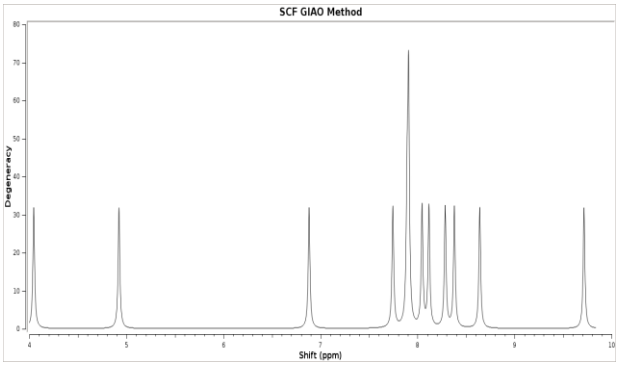

Figure 6. ^{1}H-NMR calculated spectra of aa3a dye.

Theoretical and experimental ^{13}C-NMR values of the three synthesized compounds are given in the Table 3. It is observed that all results are compatible with the synthesized structures. The numbering of the aa3c dye is given in Figure 7, and the experimental and theoretical carbon NMR spectra of the aa3a dye are given in Figure 8 and Figure 9, respectively.

Table 3. ^{13}C-NMR data for dyes aa3a-c

Carbon number	aa3a		aa3b		aa3c	
	Cal.	Exp.	Cal.	Exp.	Cal.	Exp.
C13	148.02	175.37	139.54	175.47	139.21	173.65
C19	173.16	163.63	162.66	163.55	161.45	162.66
C21	157.74	153.55	152.22	153.63	152.67	153.52
C18	162.92	152.44	158.17	152.44	158.44	151.30
C1	161.85	151.85	159.73	151.85	139.47	149.39
C10	164.98	145.36	160.98	145.31	160.96	145.31
C9	129.18	131.42	144.26	135.16	143.99	141.29
C6	137.46	130.82	132.58	131.42	132.20	131.45
C17	119.22	129.34	118.45	129.34	118.75	129.34
C24,C25	123.01	124.93	121.69	124.93	121.40	124.85
C4,C5	134.65	123.66	125.95	123.65	126.28	123.60
C22,C23	130.40	122.35	121.52	122.66	120.86	122.24
C2,C3	116.45	118.94	106.17	118.86	106.09	118.88
C16	127.06	114.02	128.03	114.42	128.01	114.55
C26	-	-	-	-	35.23	22.14

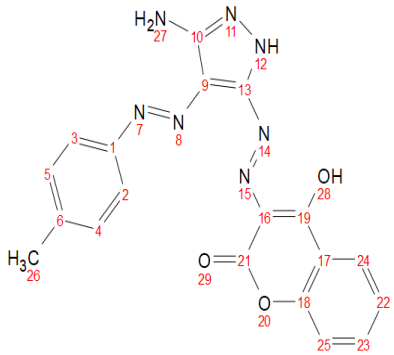

Figure 7. Numbering of atoms of aa3c dye.

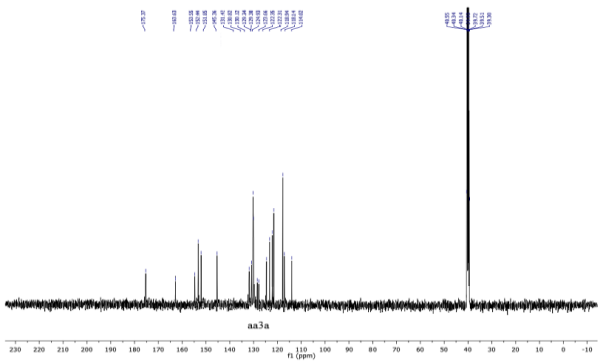

Figure 8. ^{13}C-NMR spectra of aa3a dye.

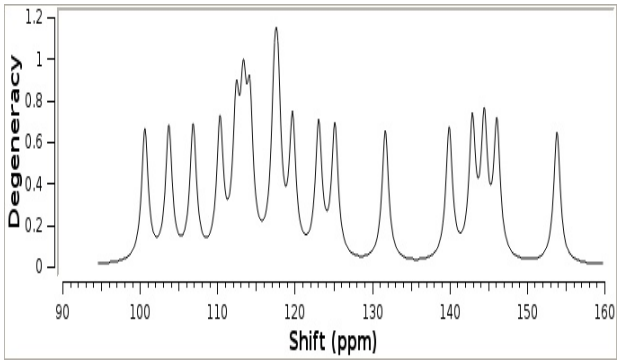

Figure 9. ^{13}C-NMR calculated spectra of aa3a dye.

3.4. Molecular electrostatic potential

The molecular electrostatic potential (MEP) at any given point around a molecule offers valuable insights into the net electrostatic effects present at that location, which arise from the complex charge distribution within the molecular system. This electrostatic profile is essential for predicting the molecule's reactivity [25,26]. The MEP surface, defined by an electron density isosurface has been carefully plotted over the optimized geometry of the cluster systems, as depicted in Figure 10. This visualization facilitates a detailed analysis of the underlying electrostatic characteristics and interactions.

As illustrated in Figure 10, this region demonstrates a high electron density attributed to the two azo groups linked to the pyrazole ring, along with the electronegative oxygen atoms present in the coumarin ring of the aa3a-c dyes. Furthermore, proton density is observed on the side of the ring that is distant from the oxygens, a consequence of the presence of these electronegative oxygen atoms in the coumarin ring.

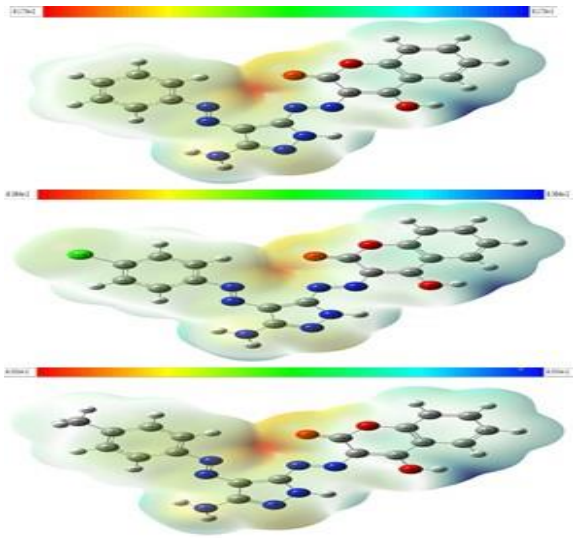

Figure 10. MEP of aa3a-c

3.5. Electronic properties

The HOMO-LUMO energy gap is an important indicator of a molecule's chemical reactivity. A smaller energy gap is indicative of lower kinetic stability in the molecule. This separation of HOMO and LUMO energies is a result of significant intermolecular charge transfer between electron donor groups and electron acceptor groups via π-conjugated pathways [27]. Furthermore, the HOMO-LUMO energy gap can also provide insights into the bioactivity associated with intramolecular charge transfer. The calculated electronic parameters for aa3a-c are presented in Table 4. HOMO-LUMO orbitals of aa3a-c dyes are given in Figure 11.

As shown in Table 4, the dye with the lowest chemical hardness is aa3a and the dye with the highest chemical softness is again aa3a. Similarly, the electron affinity and electronegativity of the aa3c dye were the highest, while this value was the lowest for the aa3b dye. These results are thought to be due to the chlorine withdrawing electrons from the ring and the methyl group donating electrons to the ring.

Table 4. Electronic properties of aa3a-c

Parameters	aa3a	aa3b	aa3c
E_{LUMO} (eV)	-5.52	-5.62	-5.81
E_{HOMO} (eV)	-3.02	-3.07	-3.22
$\Delta E = E_{LUMO} - E_{HOMO}$ (eV)	2.50	2.55	2.59
I (ionization potential) (eV)	5.52	5.62	5.81
A (electron affinity) (eV)	3.07	3.02	3.22
χ (electronegativity) (eV)	4.35	4.27	4.52
η (global hardness) (eV)	1.25	1.30	1.28
S (global softness) (eV^{-1})	0.80	0.78	0.77
μ (electronic chemical potential) (eV)	-4.27	-4.35	-4.51
ω (global electrophilicity index) (eV)	7.31	7.41	7.87

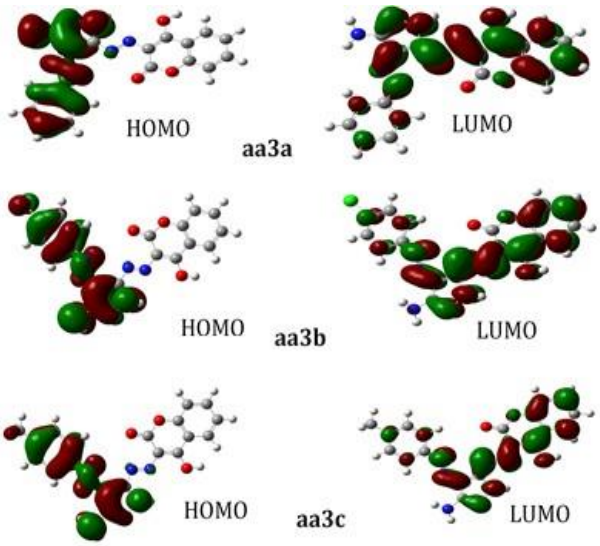

Figure 11. HOMO-LUMO orbitals for aa3a-c

As shown in Figure 11, the delocalization in the phenyl ring causes the HOMO orbitals to be concentrated in this area, while the LUMO orbitals are spread throughout the molecule.

4. Discussion and Conclusion

In our study, it is aimed to synthesize 3 heterocyclic disperse disazo dyes capable of dyeing nylon and polyester fabrics and to introduce them to the dye and textile industry. The fact that we obtain high yield products and that the end products are bright and vibrant in color confirms the content of our work.

In the continuation of the study, the structural properties of the dyes are examined and the experimental data are compared with the theoretical calculations. It is seen that the results of these comparisons are compatible with each other.

The fact that the compounds exhibit tautomeric properties and can transform from disazo-keto form in solid state to disazo-enol form in solvent shows that they may have different solubility properties. Control of the tautomeric balance can provide better binding of the dye to the target material (textile, polymer etc.) and more homogeneous distribution.

In addition, these different forms absorb light at different wavelengths, providing a wide range of colors. The change in tautomeric balance depending on environmental conditions (pH, solvent, temperature, etc.) allows the color to be adjusted and modified. This property is especially important for applications such as sensors and smart textiles.

The two azo groups linked to the pyrazole ring combined with the electronegative oxygen atoms in the coumarin ring, exhibit substantial electron density, characterizing this region as nucleophilic. In

contrast, the electrophilic area situated on the side of the rings opposite the oxygens also displays significant proton density.

In addition, electronic parameters such as hardness, softness, electron affinity, and electrophilicity index were calculated using density functional theory with values suitable for the structural properties of the synthesized aa3a-c dyes.

Based on these values, the structure with the highest electron acceptability, or the greatest tendency to attract electrons, is aa3c. Although there are minor differences, aa3a is softer than the other compounds and can be more easily polarized.

Acknowledgment

This scientific study is financially supported by Pamukkale University Scientific Research Projects Coordination Unit (grant no: 2018HZP019). I would like to thank Fikret Karcı and Gülnihal Erten for their support during this study. Also, I thank the TUBITAK/ULAKBIM clusters for their assistance in performing some computations on the Gaussian method.

Declaration of Ethical Code

In this study, we undertake that all the rules required to be followed within the scope of the "Higher Education Institutions Scientific Research and Publication Ethics Directive" are complied with, and that none of the actions stated under the heading "Actions Against Scientific Research and Publication Ethics" are not carried out.

References

[1] Said Benkhaya, Souad M'rabet, Ahmed El Harfi. 2020. Classifications, properties, recent synthesis and applications of azo dyes. Heliyon, 6, e03271.

[2] L. Abd-Alredha, R. Al-Rubaie and R. Jameel Mhessn. 2012. Synthesis and Characterization of Azo Dye Para Red and New Derivatives, e-Journal of Chemistry, 9(1), 465-470.

[3] Aykut Demirçalı, Adile Sarı. 2024. Five new heterocyclic disazo dyes derived from the 4-position: Synthesis, characterisation, and acute toxicity evaluation, Journal of Molecular Structure. 1313, 138707.

[4] V. Selvaraj, T. Swarna Karthika, C. Mansiya, M. Alagar. 2021. An over review on recently developed techniques, mechanisms and intermediate involved in the advanced azo dye degradation for industrial applications, Journal of Molecular Structure. 1224, 129195.

[5] Ehsan Ullah Mughal, Qandeel Alam Raja, Abdullah Yahya Abdullah Alzahrani, Nafeesa Naeem, Amina Sadiq, Ebru Bozkurt. 2023. Pyrimidine-based azo dyes: Synthesis, photophysical investigations, solvatochromism explorations and anti-bacterial activity, Dyes and Pigments. 220, 111762.

[6] Kamalesh Verma, Gundappa Saha, Lal Mohan Kundu, Vikash Kumar Dubey. 2019. Biochemical characterization of a stable azoreductase enzyme from Chromobacterium violaceum: Application in industrial effluent dye degradation, International Journal of Biological Macromolecules. 121, 1011–1018.

[7] Ozge Surucu, Serdar Abaci. 2018. Characterization and application of azo dye (E)-N-phenyl-4-(thiazole-2-yldiazenyl)aniline (PDA) for biomedical sterilization, Journal of the Mechanical Behavior of Biomedical Materials. 77, 408–413.

[8] Durga Prasad Mishra, Prafulla Kumar Sahu, Biswajeet Acharya, Satya Prasad Mishra, Seturam Bhati. 2024. A review of the synthesis and application of azo dyes and metal complexes for emerging antimicrobial therapies, Results in Chemistry. 10, 101712.

[9] Omer Kayir, Sevil Ozkinali. 2025. Synthesis, spectroscopic characterization and dyeing properties of new metal complexed azo dyes derived from gallic acid, Journal of Molecular Structure. 1327,141144.

[10] M.A. Castro, F.J. Pereira, A.J. Aller, D. Littlejohn. 2020. Raman spectrometry as a screening tool for solvent-extracted azo dyes from polyester-based textile fibres, Polymer Testing. 91, 106765.

[11] Alaa Z. Omar, Sara I. Nabil, Ezzat A. Hamed, Hussam Y. Alharbi, Majed S. Aljohani, Mohamed A. El-Atawy. 2025. Synthesis, characterization, and color performance of bis-azo and bis-pyrazole derivatives for dyeing of polyester, Journal of Molecular Structure. 1322, 140474.

[12] Ghulam Shabir, Jiawan Su, Aamer Saeed, and Anwar Ul-Hamid. 2021. New Heterocyclic Azo Dyes: Design, Synthesis, and Application on Leather, Fibers and Polymers. Vol.22, No.12, 3385-3392.

[13] Ghulam Hussain, Makshoof Ather, Misbah Ul Ain Khan, Aamer Saeed, Rashid Saleem, Ghulam Shabir, Pervaiz Ali Channar. 2016. Synthesis and characterization of chromium (III), iron (II), copper (II) complexes of 4-amino-1-(p-sulphophenyl)-3-methyl-5-pyrazolone based acid dyes and their applications on leather, Dyes and Pigments. 130, 90-98.

[14] H. Motiei, A. Jafari, R. Naderali. 2017. Third-order nonlinear optical properties of organic azo dyes by using strength of nonlinearity parameter and Z-scan technique, Optics & Laser Technology. 88, 68–74.

[15] Rana Forsati, Sara Valipour Ebrahimi, Keivan Navi, Ezeddin Mohajerani, Hossein Jashnsaz. 2013. Implementation of all-optical reversible logic gate based on holographic laser induced grating using azo-dye doped polymers, Optics &LaserTechnology. 45, 565–570.

[16] C. Karaca, A. Atac, M. Karabacak. 2015. Quantum chemical calculation (electronic and topologic) and experimental (FT-IR, FT-Raman and UV) analysis of isonicotinic acid N-oxide Spectrochim. Acta A 140, 85–95.

[17] Cramer, C.J., Truhlar, D.G. 2009. Density functional theory for transition metals and transition metal chemistry Phys. Chem. Chem. Phys. 11, 10757–10816.

[18] Tachibana, M., Tanak, S., Yamashita, Y. Yoshizawa, K. J. 2002. Small Band-Gap Polymers Involving Tricyclic Nonclassical Thiophene as a Building Block. Phys. Chem. B. 106, 3549–3556.

[19] Pai, C.-L., Liu, C.-L., Chen, W.-C., Jenekhe, S.A. 2006. Electronic structure and properties of alternating donor–acceptor conjugated copolymers: 3, 4-Ethylenedioxythiophene (EDOT) copolymers and model. Polymer. 47, 699–708.

[20] Zade, S.S., Bendikov, M. 2006. From Oligomers to Polymer: Convergence in the HOMO−LUMO Gaps of Conjugated OligomersOrg. Lett. 8, 5243–5246.

[21] Becke, A.D. 1988. Density-functional exchange-energy approximation with correct asymptotic behavior Phys. Rev. A. 38, 3098–3100.

[22] Lee, C., Yang, W., Parr, R.G. 1988. Development of the Colle-Salvetti correlation-energy formula into a functional of the electron density. Phys. Rev. B. 37, 785–789.

[23] Frisch, M.J., Trucks, G.W., Schlegel, H.B., Scuseria, G.E., Robb, M.A., Cheeseman, J.R.; Scalmani, G.; Barone, V.; Petersson, G.A.; Nakatsuji, H.; Li, X.; Caricato, M.; Marenich, A.V.; Bloino, J., Janesko, B.G., Gomperts, R., Mennucci, B., Hratchian, H.P., Ortiz, J.V., Izmaylov, A.F., Sonnenberg, J.L., Williams-Young, D., Ding, F., Lipparini, F., Egidi, F., Goings, J., Peng, B., Petrone, A., Henderson, T., Ranasinghe, D., Zakrzewski, V.G., Gao, J., Rega, N., Zheng, G., Liang, W., Hada, M., Ehara, M., Toyota, K., Fukuda, R., Hasegawa, J., Ishida, M., Nakajima, T., Honda, Y., Kitao, O., Nakai, H., Vreven, T., Throssell, K., Montgomery Jr., J.A., Peralta, J.E., Ogliaro, F., Bearpark, M.J., Heyd, J.J., Brothers, E.N., Kudin, K.N., Staroverov, V.N., Keith, T.A., Kobayashi, R., Normand, J., Raghavachari, K., Rendell, A.P., Burant, J.C., Iyengar, S.S., Tomasi, J., Cossi, M., Millam, J.M., Klene, M., Adamo, C., Cammi, R., Ochterski, J.W., Martin, R.L., Morokuma, K., Farkas, O., Foresman, J.B., Fox, D.J. 2016. Gaussian 16, Revision B.01, Gaussian, Inc., Wallingford CT.

[24] Dennington, R. Keith, T., Millam, J. GaussView, Version 6. Semichem Inc., Shawnee Mission, KS, 2016.

[25] Moskovits, M., DiLella, D.P. 1980. Surface-enhanced Raman spectroscopy of benzene and benzene-d6 adsorbed on silver. J. Chem. Phys. 73, 6068–6075.

[26] Moskovits, M., DiLella, D.P., Maynard, K.J. 1988. Surface Raman spectroscopy of a number of cyclic aromatic molecules adsorbed on silver: selection rules and molecular reorientation. Langmuir 4, 61–76.

[27] Diwaker and Abhishek Kumar Gupta, 2014. Quantum Chemical and Spectroscopic Investigations of (Ethyl-4-hydroxy-3-((E)-(pyrenylimino) methyl) benzoate) by DFT Method, International Journal of Spectroscopy, 841593, 15.